

Predicting soil aggregate stability using readily available soil properties and machine learning techniques

Javier I. Rivera^a, Carlos A. Bonilla^{a,b,*}

^a Departamento de Ingeniería Hidráulica y Ambiental, Pontificia Universidad Católica de Chile, Av. Vicuña Mackenna 4860, Macul, Santiago 7820436, Chile

^b Centro de Desarrollo Urbano Sustentable CONICYT/FONDAP/15110020, El Comendador 1916, Providencia, Santiago 7520245, Chile



ARTICLE INFO

Keywords:

Aggregate stability
Machine learning
Neural networks
Soil aggregates
Water-stable aggregates

ABSTRACT

Aggregate stability is a measurement of soil quality, as the presence of stable aggregates relates to a wide range of soil ecosystem services. However, aggregates stability is not reported in most soil surveys, so predictive models have been focus of increasing attention as an alternative method in the absence of direct measurements. Therefore, the objective of this study was to develop a new model for predicting aggregate stability, using two machine learning techniques: An Artificial Neural Network (ANN) model and Generalized Linear Model (GLM). These techniques were applied to a soil dataset described in terms of soil texture, organic matter content, pH, and water-stable aggregates. This dataset included 109 soil samples obtained at 0–17 cm soil depth from hyperarid, arid, semiarid, and humid regions in Chile, including agricultural soils, shrubland, and forestland. Most soil textures in this dataset were sandy loam, loam, and clay loam, and each soil property had a large range of values. Aggregate stability was measured and computed as the percentage of water-stable aggregates using a wet sieving apparatus, and the ANN and GLM models were constructed and evaluated by repeated cross-validation (80% and 20% of dataset for training and testing, respectively). The ANN and GLM models were compared by computing the modified r^2 (r_{adj}^2), Root Mean Square Error (RMSE), and Mean Absolute Error (MAE). The results demonstrated a positive gradient of aggregate stability from arid (40% in average) to humid (87% in average) regions, which is related to the increase in organic matter content and decrease in pH. Organic matter content and pH exhibited a significant correlation to the aggregate stability, with $r = 0.56$ and $r = -0.73$, respectively. Moreover, among the fractions used to compute the soil texture, the clay content exhibited the highest correlation with aggregate stability ($r = 0.30$). These variables were used for training and testing the ANN and GLM models. The ANN model achieved superior performance in terms of the RMSE, (r_{adj}^2) and MAE in the cross-validation procedure, and showed $r^2 = 0.80$ for training and $r^2 = 0.82$ for testing. The GLM yielded $r^2 = 0.59$ and $r^2 = 0.63$ for training and testing, respectively. Therefore, despite the limitations observed when implementing ANN, its use is recommended instead of GLM as a reference model. Considering the small number of easily measured variables, this study provides two models that can be coupled with other existing soil routines or can be used directly to complete soil surveys where the aggregate stability was not measured.

1. Introduction

Soil is the primary component of terrestrial ecosystems, and its degradation leads to a decrease in soil capability to provide ecosystem services. One of the most important indicators for soil degradation is aggregate stability (An et al., 2010; Deviren Saygm et al., 2012). Resistance of aggregates to breakdown affects a wide range of soil processes and properties such as soil compaction, soil organic matter stabilization and organic carbon protection from erosion or decomposition, microbial community structure, nutrient adsorption,

infiltration, hydraulic conductivity, aeration, root development, seed germination, soil susceptibility to surface runoff and interrill erosion, and crusting (Le Bissonnais, 1996; Wright and Upadhyaya, 1998; Amézketa, 1999; Chenu et al., 2000; Six et al., 2004; Abiven et al., 2008; Duchicela et al., 2013; Chaplot and Cooper, 2015; Shahbaz et al., 2017). Hence, the presence of topsoil stable aggregates is crucial for maintaining soil productivity, enhancing carbon sequestration, promoting nutrient cycling, and minimizing vulnerability to water erosion (Bronick and Lal, 2005; Chaplot and Cooper, 2015). Thus, there has been increasing interest in quantifying its spatial variability or

* Corresponding author at: Departamento de Ingeniería Hidráulica y Ambiental, Pontificia Universidad Católica de Chile, Av. Vicuña Mackenna 4860, Macul, Santiago 7820436, Chile.

E-mail address: cbonilla@ing.puc.cl (C.A. Bonilla).

developing spatial predictions using geostatistical techniques (Mohammadi and Motaghian, 2011; Annabi et al., 2017). Moreover, as aggregate stability is a crucial factor for understanding soil potential, it is used as a predictor in environmental models and computer routines when estimating the soil erosion, organic carbon sequestration, infiltration, and soil water retention (Cantón et al., 2009; Chaplot and Cooper, 2015; Rahmati et al., 2017; Xiao et al., 2017; Haghverdi et al., 2018).

Soil aggregation is a complex process involving dynamic interaction of the soil organic materials and mineral composition, resulting in the inception of a microaggregate (< 0.25 mm) within a macroaggregate (Angers et al., 1997; Six et al., 2004). Previous studies have indicated that general soil properties closely related to soil aggregate stability are soil texture, organic matter content, polyvalent cations in the soil solution, pH, and microbial activity (Six et al., 2004; Dimoyiannis, 2012; Regelink et al., 2015). Soil properties responsible for soil aggregation are related to the aggregate size (Almajmaie et al., 2017). Soil organic matter acts as the main binding agent of the soil primary particles in aggregate formation and stabilization of slaking resistant macro-aggregates, while mineralogy, cation ratios, and cementing agents are strongly associated with microaggregate stability (Bronick and Lal, 2005; Mohammadi and Motaghian, 2011; Duchicela et al. 2013; Paul et al., 2013). In this dynamic aggregation process, clay particles act as binding agents forming organo-mineral assemblages during interaction with the soil organic matter, thereby reducing the aggregate wettability and influencing the mechanical strength of soil aggregates (Onweremadu et al., 2007; Regelink et al., 2015).

To date, different approaches have been developed to measure and characterize soil aggregation. Aggregate stability is usually measured by wet sieving methods and computed as water-stable aggregates (WSA), in which aggregates are raised and lowered cyclically above a sieve immersed in water. With this aim, several methodologies have been developed, which differ in the limit of the aggregate sizes, the use of a single or set of sieves with varying mesh sizes, and the intensity of the disruptive mechanical energy used in the process (Le Bissonnais, 1996; Pulido Moncada et al., 2013; Belaid and Habaieb, 2015). However, no general agreement or standard method exists for the determination of aggregate stability (Mataix-Solera et al., 2011). Moreover, the majority of methods are time consuming and expensive; therefore, these measurements are rarely included in soil analysis routines (Cañasveras et al., 2010; Mataix-Solera et al., 2011). Hence, an alternative solution for generating such data is estimating the aggregate stability by using predictive models. Table 1 presents a review of the main predictive models for aggregate stability.

Over the past several decades, pedotransfer functions (PTFs) have been used for predicting several soil properties. PTFs that translate

simpler soil data into soil aggregate stability estimates have been derived by different methods, from simple linear regression to advanced machine learning techniques (Lagos-Avid and Bonilla, 2017; Contreras and Bonilla, 2018). Tisdall and Oades (1982) reported the use of soil organic matter as a main predictor by using linear regression (Table 1). Bazzoffi et al. (1995) used a dataset of 15 soils from the sub-Appenine region in north-central Italy to develop three linear regressions based on sand and clay fractions, iron and aluminum oxides, and calcite, chlorite, and feldspar, respectively (Table 1). Cañasveras et al. (2010), Tavares Filho et al. (2012), Gomez et al. (2013), and Wu et al. (2017) also developed linear regressions, but in addition to organic matter, used other predictors such as bulk density, clay content, pH, resistance to penetration, particle density, soil mechanical resistance, free iron oxides, cation exchange capacity, sesquioxides, and pore size distribution (Table 1). Furthermore, two logarithmic fits were proposed by Mataix-Solera et al. (2010), using organic matter content as input. Recent developments in artificial intelligence methods have enabled several studies to predict aggregate stability using machine learning techniques, such as the adaptive neuro-fuzzy inference system, artificial neural networks (ANN), and support vector machines techniques (Table 1). These PTFs are mainly based on soil texture, organic matter content, cation exchange capacity, normalized difference vegetation index (NDVI), and iron content (Table 1) (Besalatpour et al., 2012, 2013; Erktan et al., 2016; Annabi et al., 2017).

Best PTFs for predicting soil aggregate stability require the use of at least one of the following techniques: diffuse infrared spectroscopy, laser granulometry, reflectance spectroscopy, inductively coupled plasma optical emissions spectroscopy, X-ray fluorescence, topographic information with a 20×20 m digital elevation model, soil mechanical resistance, or soil penetration resistance (Bazzoffi et al., 1995; Cañasveras et al., 2010; Tavares Filho et al., 2012; Besalatpour et al., 2013; Gomez et al., 2013; Annabi et al., 2017; Wu et al., 2017; Erktan et al., 2016). However, simpler PTFs such as those developed by Tisdall and Oades (1982), and Besalatpour et al. (2012) are restricted to red-brown earth soils and soils dominated by calcareous materials, respectively. Therefore, no universal model exists for predicting aggregate stability that is capable of reflecting a wide range of soil types and local conditions (Annabi et al., 2017). Despite the extensive advances in developing PTFs for estimating aggregate stability, further exploration in using the minimum number of readily available soil properties as inputs for estimating aggregate stability is required.

From this perspective, the use of machine learning techniques such as Artificial Neural Networks (ANN) has been demonstrated to be one method with superior estimates, and it is recognized for its capability of modeling complex and nonlinear relationships (Xu et al., 2017). The training process for the ANN algorithm is similar to the nature of the

Table 1
Summary with the main aggregate stability models.

Reference	Model input	Expression for aggregate stability
Tisdall and Oades (1982)	Organic matter content	% water slaking
Bazzoffi et al. (1995)	Chemical properties: FeO and TiO ₂ Mineralogical properties: Calcite, chlorite, and feldspar Physical properties: Sand and clay contents	MDW
Cañasveras et al. (2010)	Texture, pH, organic matter content, Fe, calcium carbonate, and spectral principal components	MDW
Mataix-Solera et al. (2010)	Organic matter content	WSA
Tavares Filho et al. (2012)	Clay, bulk density, penetration resistance, pH, and organic matter content	WSA, MDW, WDC
Besalatpour et al. (2012)	Texture, organic matter content, slope, aspect, NDVI, elevation, and cation exchange capacity	WSA
Besalatpour et al. (2013)	Organic matter content, clay, cation exchange capacity, slope, aspect, and NDVI	GMD
Gomez et al. (2013)	Clay, free iron, organic carbon content, pH, cation exchange capacity, calcium carbonate, and visible near infrared spectra	MDW
Erktan et al. (2016)	Infrared spectroscopy and laser granulometry	MWD
Wu et al. (2017)	Clay, organic matter content, forms of sesquioxides, and pore size distribution	FW, WS, SW
Annabi et al. (2017)	Soil texture, total carbon and nitrogen content, iron, CaCO ₃ , salinity, CEC, and pH	MDW

MDW: Mean weighted aggregate diameter. WSA: Water stable aggregates. WDC: Water dispersible clay. IeaE: Aggregate stability index. FW: Fast wetting. WS: Wet stirring. SW: Slow wetting.

human brain, as it consists of a set of interconnected units or neurons, organized in input, hidden, and output layers (Tamari et al., 1996). Moreover, compared to machine learning techniques such as ANN, linear regression methods have been preferred for developing PTFs owing to their advantages in terms of computational efficiency, relatively ease of use, and interpretability (Minasny and Hartemink, 2011). Thus, it is highly convenient to develop and evaluate the PTFs generated by ANN and Generalized Linear Model (GLM) techniques, using GLM as a benchmark or control method. Furthermore, when comparing and evaluating PTFs, the most common and standard resampling method has been cross-validation, because this approach maximizes the data availability and generates accuracy metrics (Wösten et al., 2001; Deng et al., 2018).

Therefore, the main objective of this study was to build a reliable PTFs for estimating soil aggregate stability by using ANNs and GLM techniques from typically measured soil properties. With this purpose, a soil aggregate stability dataset was prepared based on soil physical-chemical properties and the percentage of WSA, using a wet sieving apparatus. Correlation analysis was used to identify the main variables controlling the aggregate stability, and the PTFs generated by means of the ANN and GLM techniques were compared using the soil aggregates dataset. A comparison of the models was conducted with an internal cross-validation procedure, while the predictions were tested with an independent set of soil samples. Finally, the developed PTFs were compared with existing PTFs in terms of their reliability.

2. Materials and methods

2.1. Soil samples and soil properties

In order to obtain a wide range of values for the soil properties used in this study, the sampling area covered different soil types, land uses, and climatic conditions. A total of 109 soil samples were obtained at a

0–17 cm depth, distributed between latitudes of 27°43'S and 51°20'S in Chile (Fig. 1). The study area was located in four of the eight Chilean soil zones, namely desert (19 sites), arid Mediterranean (37 sites), wet Mediterranean (30 sites), and Magellan (23 sites) (Luzio et al., 2010; Ramírez et al., 2019). The climate range in the study area varies from hyperarid to humid. In terms of rainfall, the desert zone is classified as hyperarid, with 43 mm y^{-1} of rainfall, while that in the arid Mediterranean zone does not exceed 440 mm y^{-1} (Bonilla and Vidal, 2011; Uribe et al., 2012). In contrast, the wet Mediterranean and Magellan zones are classified as humid, with 1220 mm y^{-1} and 238 mm y^{-1} rainfall, respectively (Uribe et al., 2012). The soil orders in the study were Alfisols, Andisols, Histosols, Inceptisols, Mollisols, and Ultisols, where Andisols increases its presence from the Mediterranean to Magallan zones (Casanova et al., 2013). Soil samples in the desert, arid, and wet Mediterranean zones were mainly located in the central valley, which includes most cultivated soils and concentrates most of the productive land in the country, scrubland, and forest areas (INE, 2007; Bonilla and Johnson, 2012). However, Magellan zone soils are located in the Serrano river basin, in which the dominant vegetation is native forest, bushes, and peaty scrubland (Bonilla et al., 2014; Carkovic et al., 2015; González et al., 2016).

2.2. Soil sample analysis

Soil samples were dried at 40 °C and sieved at ≤ 2 mm. The sieved fraction was used to determine the organic matter (OM) content by oxidation with a mixture of dichromate and sulfuric acid (Nelson and Sommers, 1996), particle size distribution (clay, silt, and sand) with the pipette method (Gee and Bauder, 1986), and pH with a 1:2.5 soil: water suspension.

The aggregate stability was measured using a wet sieving apparatus (Eijkelkamp Agrisearch Equipment, Giesbeek, The Netherlands) according to the methodology described by Kemper and Rosenau (1986),

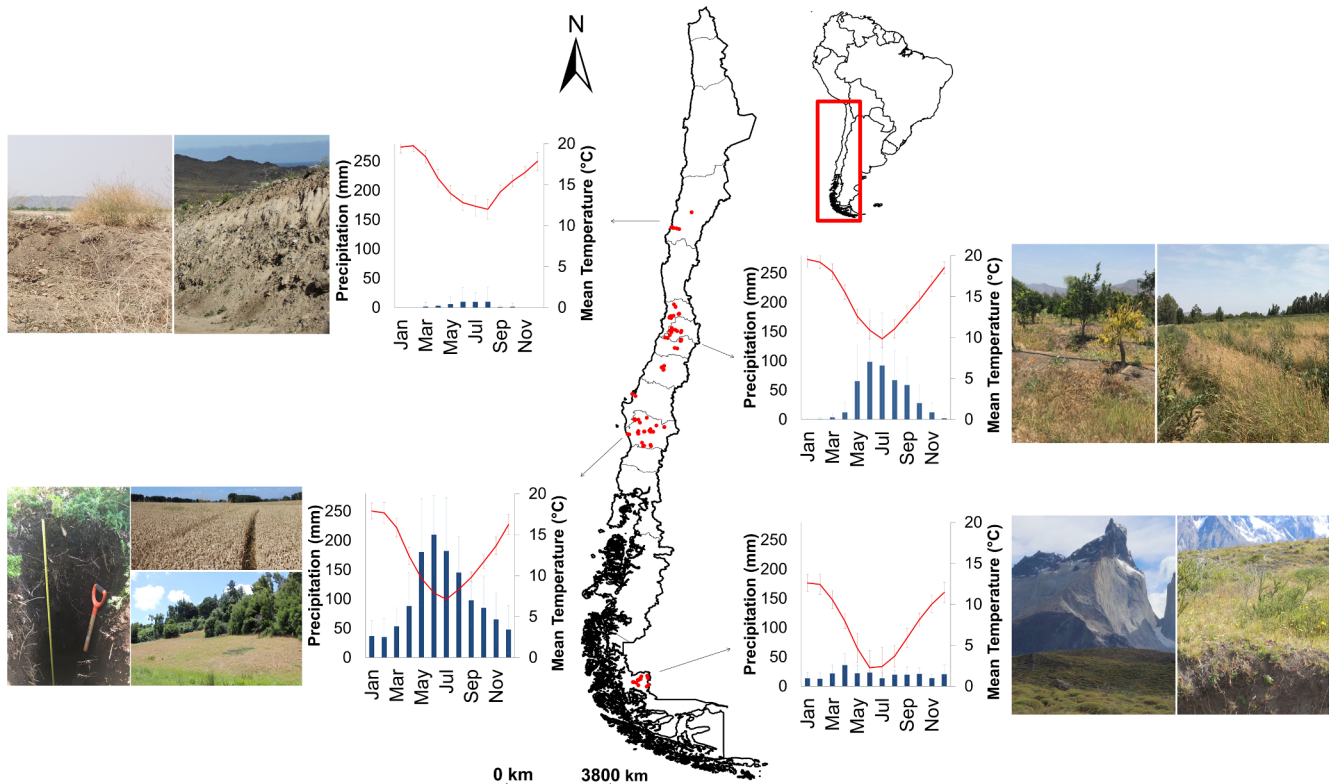


Fig. 1. Study area location. The red dots indicate the sampling sites, which are distributed in four zones consisting of hyperarid, arid, semiarid, and humid climates. Each zone is displayed alongside a climograph and representative characteristics image. (For interpretation of the references to colour in this figure legend, the reader is referred to the web version of this article.)

which emphasizes the principle that unstable aggregates break down when immersed in water. The wet sieving methodology used involves aggregate breakdown via slaking and mechanical dispersion, which is a primary mechanism of aggregate dispersion (Annabi et al., 2017), and emulates the stresses involved in the entry of water into the soil aggregates in the field. According to Kemper and Rosenau (1986), 4.0 g of 1–2 mm dried aggregates were placed in a sieve of 0.25 mm, which were raised and lowered in the distilled water for 3 min. During these 3 min of wet sieving, unstable aggregates passed through the sieve and were collected in the distilled water-filled can underneath the sieve. Thereafter, the cans were replaced and filled with a dispersing solution (sodium hexametaphosphate for soils with pH > 7 and sodium hydroxide for soils with pH < 7), and the sieving continued until sand particles and small root fragments remained on the sieves. Then, both sets of cans, filled with distilled water and dispersing solution, respectively, were dried at 110 °C until the water was evaporated. Finally, the weight of unstable aggregates was determined by weighing the can filled with water plus their contents, and subtracting the weight of the can, while the weight of stable aggregates was determined by weighing the can filled with dispersing solution plus their contents, and subtracting the weight of the can and 0.2 g of the dispersing solution. Then, the WSA index was calculated as the percentage of stable aggregates by dividing the weight of the stable aggregates obtained in the dispersing solution cans over the sum of the weights of the stable and unstable aggregates (Eq. (1)), in which 100% indicated that none of the aggregates were broken, while 0% indicated that the totality of aggregates were broken.

$$\text{WSA} = (\text{W}_{\text{ds}}/\text{W}_{\text{ds}} + \text{W}_{\text{dw}}) \cdot 100 \quad (1)$$

where WSA is the index of water-stable aggregates (%), W_{ds} is the weight of aggregates dispersed in the dispersing solution (g), and W_{dw} is the weight of aggregates dispersed in distilled water (g).

2.3. Machine learning techniques

Two contrasting machine learning techniques were used for deriving the PTFs for predicting the aggregate stability. First, the GLM model was developed using the `glm` R Package (Guisan et al., 2002; R Core Team, 2018). In the GLM model, predictor variables X_j , ($j = 1, \dots, n$) were combined to produce a linear predictor related to the expected value $\mu = E(Y)$ of the response variable (dependent) Y by fitting a linear regression equation to the measured dataset (McCullagh and Nelder, 1989). Thus, the GLM model had the following form:

$$E(Y) = \alpha + \sum_{i=1}^n X_i \beta_i \quad (2)$$

where Y denotes the dependent variable, α is a constant known as the intercept, $X = (X_1, \dots, X_n)$ is a vector of explanatory variables, and $\beta = (\beta_1, \dots, \beta_n)$ is a vector of regression coefficients for each explanatory variable.

The ANN model was developed using the logistic function in the `neuralnet` R Package (Günther and Fritsch, 2010; R Core Team, 2018). The equation describing the output (Y_k) of the neuron k in the hidden layer was as follows:

$$Y_k = f\left(\omega_k + \sum_{i=1}^n \omega_{ki} x_i\right) \quad (3)$$

where ω_k is the intercept of the output neuron k ; ω_{ki} is the connection weight between the output neuron k and hidden neuron i ; x_i is the output from neuron i in the hidden layer; n is the number of neurons in the hidden layer; and f is the activation function.

It is recognized that one disadvantage of ANN techniques relates to their “black box” nature and limited capacity to identify possible causal relationships. In order to overcome these limitations, the contribution of the input variables in predicting the aggregate stability was evaluated by computing the relative importance (RI) parameter, as

described by Olden and Jackson (2002).

2.4. Evaluation of PTFs

The caret package in R was used to compare the PTFs derived using the GLM and ANN methods with a repetitive cross-validation procedure, using soil texture, organic matter content, and pH as inputs for predictive models (Heung et al., 2016). In the cross-validation procedure, a standard 80% (i.e. $n = 87$) of the entire data set was used as training and randomly partitioned into 10 subsets (Wösten et al., 2001; Forkuor et al., 2017). One subset was excluded exactly once as a validating set and the PTFs were trained on the remaining subsets, following which the root-mean-square error (RMSE), adjusted r^2 (r_{adj}^2), and mean absolute error (MAE) were averaged over 10 iterations (Heung et al., 2016). In order to avoid over-fitting, five repetitions were carried out in the cross-validation procedure. Thus, 50 RMSE and MAE values were obtained for each method. The GLM and ANN were compared by computing the average of the errors over all cross-validation repetitions, and a paired *t*-test was used to determine significant differences. Moreover, in order to compare the model precision with that of previous studies, the relative RMSE (RMSE/\bar{O} , where \bar{O} is the mean of observed values) was also computed. Based on Li et al. (2013), a model is excellent, good, fair, and poor when the relative RMSE is less than 10%, 20%, 30% or more than 30%, respectively. Finally, the PTFs were tested with the remaining 20% of the entire dataset (i.e. $n = 22$), and the coefficient of determination (r^2) was computed (Forkuor et al., 2017; Kuhn, 2018). The RMSE and MAE statistics were computed as follows:

$$\text{RMSE} = \sqrt{\frac{1}{n} \sum_{i=1}^n (P_i - O_i)^2} \quad (4)$$

$$r_{\text{adj}}^2 = 1 - \frac{(\sum_{i=1}^n (P_i - \bar{O})^2)/(n - k)}{(\sum_{i=1}^n (O_i - \bar{O})^2)/(n - 1)} \quad (5)$$

$$\text{MAE} = \frac{1}{n} \sum_{i=1}^n |P_i - O_i| \quad (6)$$

where O_i and P_i are the observed and predicted aggregate stabilities, respectively, \bar{O} is the mean of the observed values, k is the total number of explanatory variables, and n is the amount of values.

3. Results and discussion

3.1. Soil properties

Nine out of the 12 USDA soil texture classes were identified in the study area (Fig. 2). The majority of samples were concentrated in three textural classes: sandy loam, loam, and clay loam. Table 2 displays the high variability in the soil properties across the study area. Moreover, a positive gradient of aggregate stability from the desert to Magellan zones was observed. This trend relates to the increase in the OM content and presence of Andisols from the Mediterranean zone to Magellan zones. Andisols and OM content promote a decrease in water dispersion of aggregates by avoiding air slaking, and improve aggregate formation and stabilization (Karami et al., 2012; Casanova et al., 2013).

Fig. 3 illustrates the relationship between the measured soil properties and WSA. The trends indicate that an increase in OM and clay contents contributed to the soil aggregate stability. Moreover, based on the correlation analysis, the most important soil properties affecting the aggregate stability were OM, pH, and clay content with correlation coefficients of 0.56, -0.73, and 0.3, respectively. On the other hand, there was a slight relationship between the WSA and sand and silt fractions, with correlation coefficients of -0.09 and -0.17, respectively. These results are consistent with previous studies that reported the relevance of clay and OM in the aggregate stabilization process

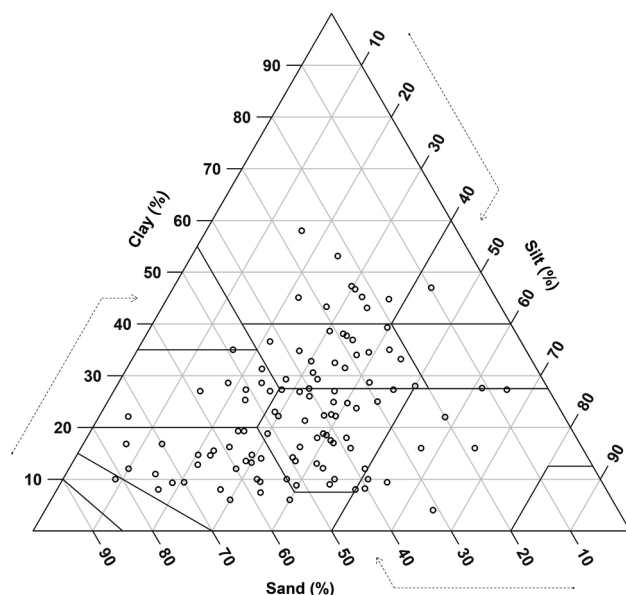


Fig. 2. Soil texture triangle for the soil samples used in this study ($n = 109$).

Table 2
Statistical summary of soil sample properties.

Property	Mean	Standard deviation	Minimum	Maximum
Sand (%)	43.4	16.2	7.4	81.2
Silt (%)	34.1	12.6	4.9	66.0
Clay (%)	22.9	11.9	4.0	58.0
OM (%)	6.5	5.2	1.0	22.8
pH	6.7	1.1	4.7	8.8
WSA (%)	73.4	19.8	12.5	98.7

OM: organic matter content; WSA: water-stable aggregates.

(Abiven et al., 2008; Idowu, 2003). The main binding agents forming organo-mineral assemblages are clay particles and OM, which are influenced by polyvalent cations and their solubilities and mobilities, that depend on soil pH (Tisdall and Oades, 1982; Six et al., 2004; Bronick and Lal, 2005; Igwe et al., 2009; Almajmaie et al., 2017). Hence, the interaction between clay and OM with soil aggregates is affected by soil pH.

Regarding to the decrease in WSA with an increasing pH, the dispersion of aggregates by water is substantially stronger at high pH values. Previous studies demonstrated that aggregate stability increases with a decrease in pH. At low pH values (< 7), microbial activity increases, which promotes macroaggregation and stabilization. Moreover, the solubility and mobility of cations are higher, and these form bridges with the clay and soil OM (Tisdall and Oades, 1982; Schutter and Dick, 2002; Bronick and Lal, 2005; Regelink et al., 2015; Wu et al., 2017). At pH values > 7, the pH relates to cementing agents such as calcium carbonate (Weng et al., 2011). However, according to the aggregate classification by size, this cementing agent type is strongly associated with the stability of microaggregates (Amézketa, 1999; Nciizah and Wakindiki, 2015; Almajmaie et al., 2017). As mentioned in the methodology section, this study evaluated aggregates using water as a dispersing agent, with a mesh size corresponding to macroaggregates. Therefore, the effect of this cementing agent at high pH values cannot be evaluated.

3.2. Aggregate stability estimates

The performances of the GLM and ANNs models were evaluated comparing the RMSE, r^2_{adj} , and MAE, and the t-tests indicated significant differences at the 0.05 level between the models in each error metric

(Fig. 4). The ANN PTFs performed better than the GLM functions, in terms of the RMSE, r^2_{adj} , and MAE, with mean values of 10.1, 0.78, and 9.7, respectively. Meanwhile, the GLM and ANN models provided relative RMSE values of 11.8 and 16.5, respectively, performing as good models according to the categories described by Li et al. (2013). As expected, the results obtained demonstrated that ANN techniques offer high predictive power, as indicated in previous studies (Besalatpour et al., 2013). This is because ANNs techniques are suitable for modeling and detecting complex nonlinear relationships between dependent and independent variables, in which GLM is limited (Forkuor et al., 2017; Krishnan et al., 2018).

As expected, the predictors with significant levels (0.05 and 0.01) in the correlation analysis (Fig. 3); that is, OM, pH, and clay, provided superior PTFs using the GLM method, with $r^2 = 0.59$ in the training dataset. The GLM model is expressed as follows:

$$\text{WSA (\%)} = 122.4 + 1.1 \cdot \text{organic matter} + 0.19 \cdot \text{clay} - 9.1 \cdot \text{pH} \quad (7)$$

where WSA is the index of water stable aggregates (%), OM is organic matter content (%), clay content (%), and soil pH.

The obtained coefficients for OM content and clay in Eq. (7) are positive as these are the main variables forming organo-mineral assemblages in the aggregate formation and stabilization process (Regelink et al., 2015). On the other hand, the coefficient for pH is negative and higher than those for the other variables, which is consistent with the order of magnitude of the identified correlations. This reflects the pH influence on the solubility and mobility of cations, which forms bridges between clay and OM particles, with a higher solubility at a low pH (Bronick and Lal, 2005).

The resulting ANN contains three neurons and five input variables: sand, silt, clay, OM content, and pH. Most of the relationships in the ANN are not linear, so using all the soil fractions (sand, silt, and clay) gives different weights to each one, improving the model estimates. This same approach has been used in Besalatpour et al. (2012), Cañasveras et al. (2010), and Lagos-Avid and Bonilla (2016).

The weights of each connections between neurons and the ANN structure are illustrated in Fig. 5. The normalized X_i inputs ($X - X_{\min}/X_{\max} - X_{\min}$) for the neuron k ($k = 1-5$) are multiplied by the weights W_{ki} and summed together with the constant bias term. The resulting is the input for the sigmoid function ($f(u) = \frac{1}{1+e^{-u}}$), which produces the input for the output layer which are multiplied by LW_j and summed together with the constant term to form the output Y (Eq. (8)). Finally, this output is normalized and must be reverse-processed in order to obtain the estimated WSA values. The ANN model is expressed as follows:

$$Y = \sum_{k=1}^3 LW_j \text{sigmoid}\left(b_k^1 + \sum_{i=1}^5 W_{ki} X_i\right) + b_1^2 \quad (8)$$

where W_{ki} is the connection weight between the hidden neuron k and the input i , X_i is the normalized input i , b_k^1 is the constant bias term of hidden neuron k in the hidden layer, b_1^2 is the constant bias term in the output layer, LW_j is the connection weight between the hidden neuron j and the output Y .

The relative input weights in the ANN model indicate that OM content is the most important input (RI = 40%). As mentioned previously, the OM content was found to be highly correlated to the aggregate stability. In contrast, sand only exhibited RI = 6%. Among the other inputs, clay, pH, and silt yielded RI values of 8%, 11%, and 35%, respectively. Consequently, in the ANN model, the aggregate stability was mainly controlled by the soil texture and OM content.

The PTFs obtained using the GLM and ANNs techniques were tested with the remaining independent data (20%). In this analysis, the GLM PTFs exhibited lower precision compared to those of the ANN. Low WSA values (between 13% and 20%) were overestimated in the testing as well as in the entire dataset with the GLM model (Fig. 6). The

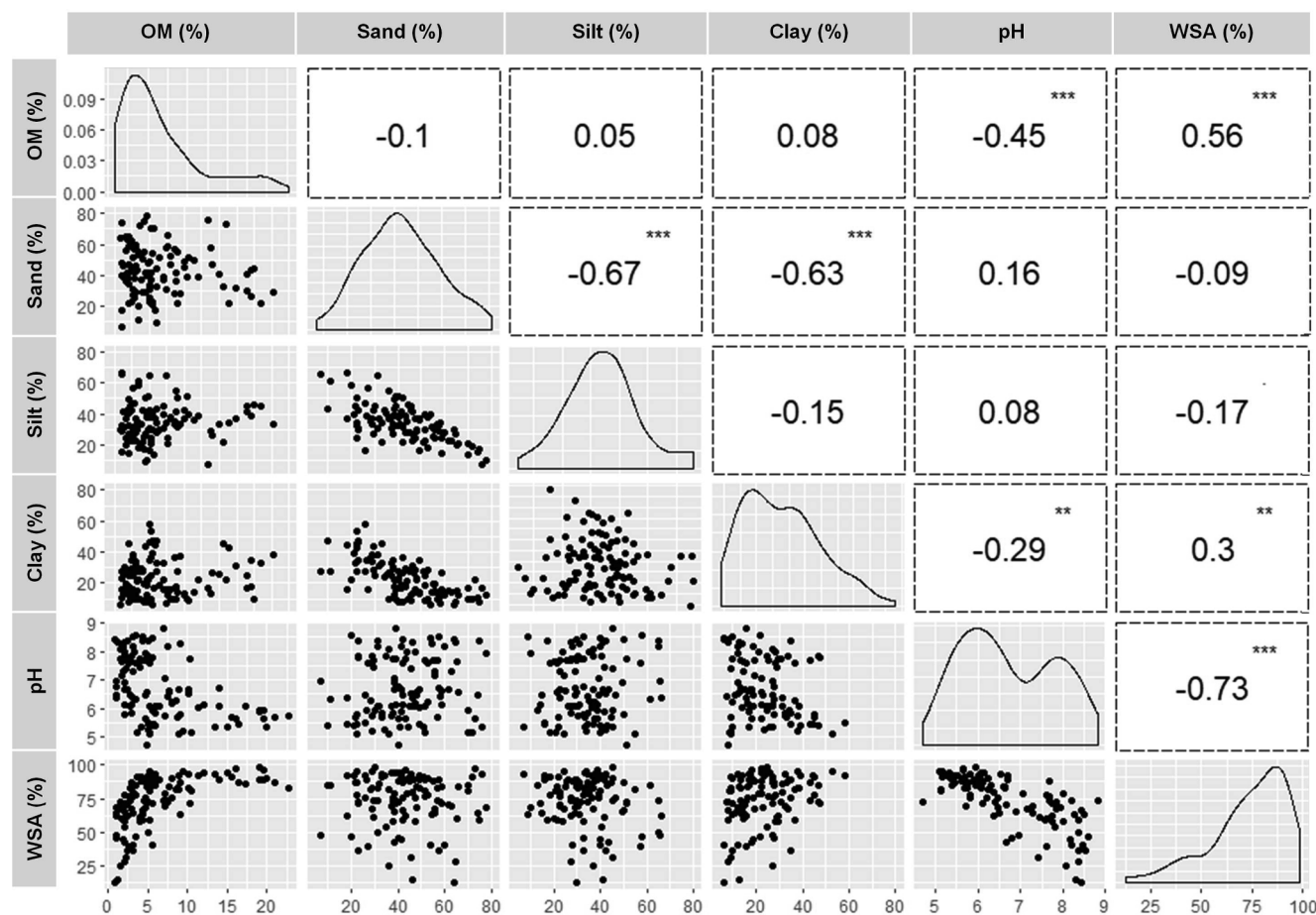


Fig. 3. Scatterplot matrix illustrating relationships among soil properties used in this study. A density plot is indicated in the diagonal. Pairwise scatter plots between variables are displayed below the diagonal (e.g. organic matter vs. WSA is plotted in the final row and first column). The linear correlation values are indicated above the diagonal (significant at *: 0.01. **: 0.1, ***: 0.05). OM: organic matter content; WSA: water-stable aggregates.

datasets used for training and testing indicated close statistical values to the entire dataset (Table 3). Thus, according to this comparison, the ANN model was superior for predicting aggregate stability. Consequently, despite the limitations regarding to computational efficiency and implementation facilities, the ANN model is recommended, as opposed to the GLM used as a benchmark in this study.

3.3. Comparison with other aggregate stability models

Previous studies on soil aggregate stability differed, in terms of either the measurement or approaches used for the model training and testing. Therefore, it is difficult to conduct a fair and direct comparison. However, in order to compare the model capabilities, we computed the mean r^2 value for two model types. For the first type, which consisted of models that were restricted because they were constructed with a

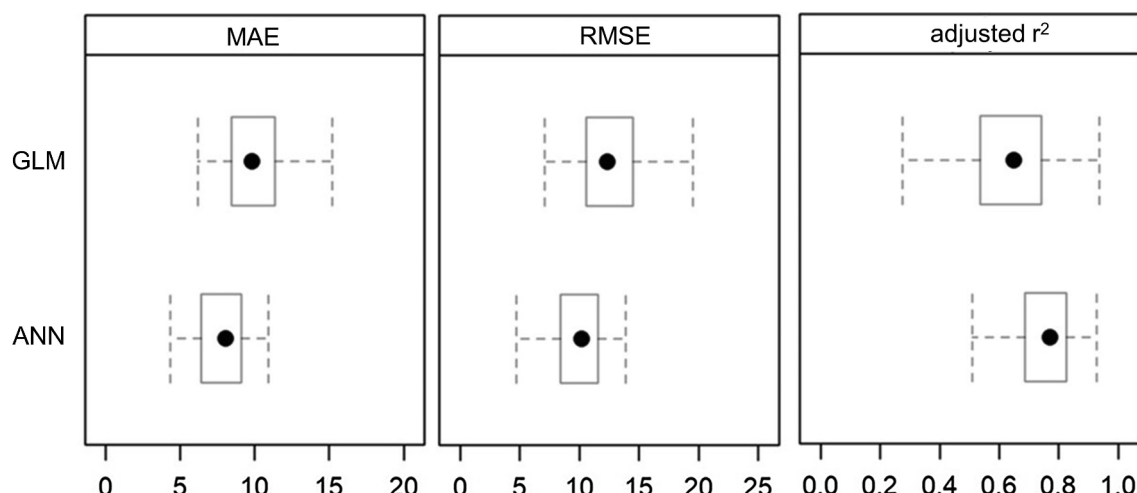


Fig. 4. Boxplots for MAE, RMSE, and adjusted r^2 for cross-validation procedure based on 80% of dataset. Error bars are 95% confidence intervals.

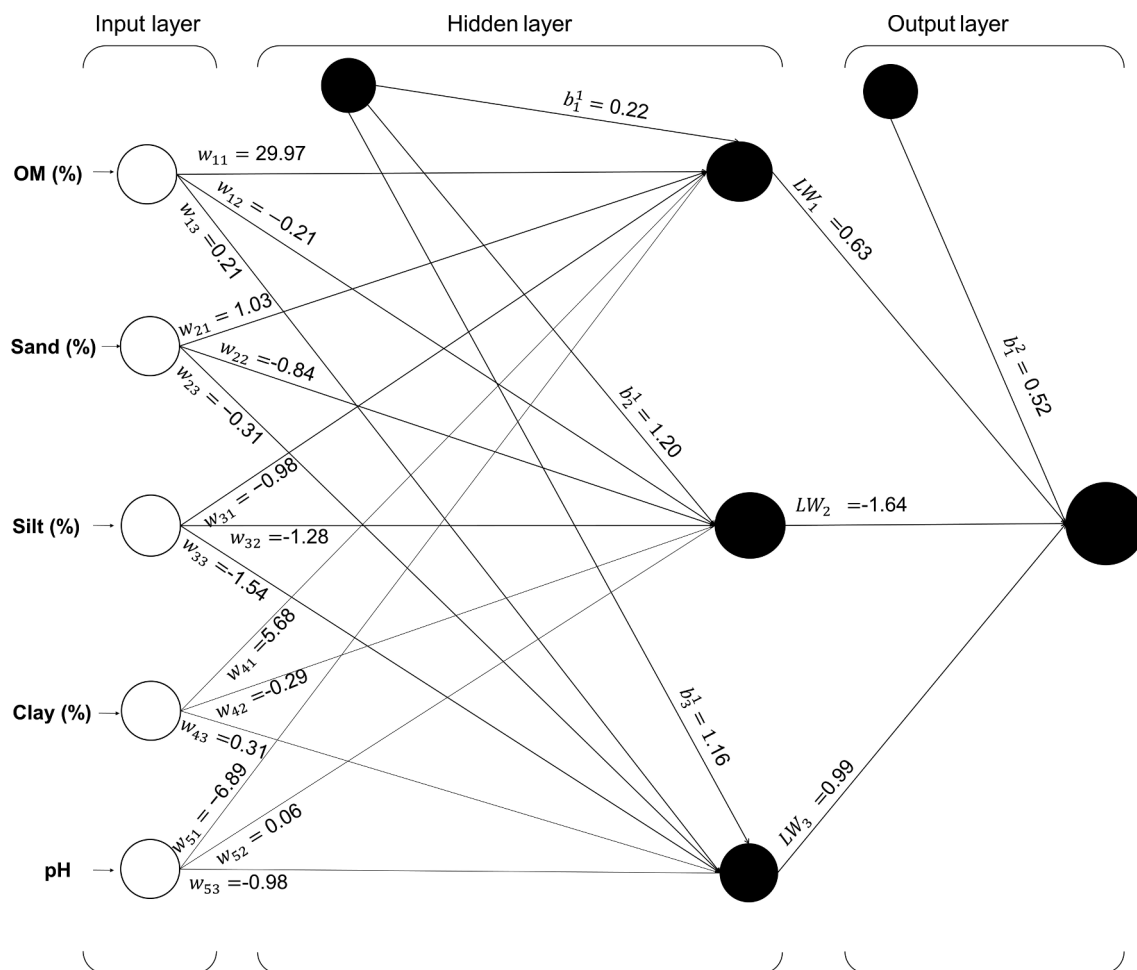


Fig. 5. ANN model diagram and connection weights for predicting soil aggregate stability.

limited and local dataset (Tisdall and Oades, 1982; Mataix-Solera et al., 2010; Besalatpour et al., 2012), the average reported r^2 was 0.58. For the second type, which included models requiring more expensive predictors (Bazzoffi et al., 1995; Cañasveras et al., 2010; Gomez et al., 2013; Erktan et al., 2016; Annabi et al., 2017; Wu et al., 2017), the average reported r^2 was 0.81. The GLM and ANN models developed in this study exhibited higher r^2 values than the first type of models, at 0.80 and 0.82 for the training and testing, respectively. When comparing to the second type, only the ANN model was superior in testing ($r^2 = 0.82$), while the GLM was only superior in testing ($r^2 = 0.63$).

One of the main advantages of the GLM and ANN models is the wide range of values in soil properties that are used as predictors compared to preceding models. Tavares Filho et al. (2012) and Gomez et al. (2013) used pH values ranged in mainly basic and only acid soils, respectively. In contrast, the GLM and ANN models in this study were constructed using pH values from 4.7 to 8.8 (Table 2). Moreover, in this study, a total of 109 soil samples were used, compared to the 15 and 12 samples used in the studies of Bazzoffi et al. (1995) and Wu et al. (2017), respectively. Furthermore, Cañasveras et al. (2010), Erktan et al. (2016), and Annabi et al. (2017) used predictors requiring special devices and highly skilled technicians. In contrast, the GLM and ANN models use readily available data as input (texture, OM content, and pH).

Finally, when comparing to similar previous studies such as Mataix-Solera et al. (2010), that study reported WSA estimates with an $r^2 = 0.27$ using a logarithmic equation with OM content as predictor. We evaluated this equation, and first we predicted the entire WSA dataset developed in our study and obtained $r^2 = 0.42$. Thereafter, in

order to improve the prediction accuracy, the original parameters were fitted with the entire dataset, but only a slight improvement was achieved ($r^2 = 0.45$). Thus, the quality of the estimates was lower than that of the GLM and ANN models, which had $r^2 = 0.60$ and $r^2 = 0.80$ for the entire dataset, respectively.

4. Conclusions

The aggregate stability exhibited a significant and positive relationship with OM and clay contents, and a negative relationship with pH. The cross-validation used in this study to develop the GLM and ANN models indicated that the ANN PTFs performed better than the GLM, with $r^2 = 0.80$ for the entire dataset.

As a result of the wide range of soils and soil properties found in the study area, the GLM and ANN models developed in this study provide an alternative for other areas with limited soil data in the absence of soil aggregate measurements. Although several previous studies have reported higher accuracy, most of these were based on a limited dataset or used soil predictors requiring special techniques that are not always available.

Finally, this study demonstrated that using readily available soil input data is possible to develop a reliable model for predicting soil aggregate stability. Moreover, owing to the different characteristics of the GLM and ANN models, this study provides PTFs for users with different modeling skills. In addition, these models can be used and applied to guide strategies for soil evaluation and conservation, either by direct computing of the aggregate stability or by implanting the equations in certain of already existing soil physics or soil hydrology models.

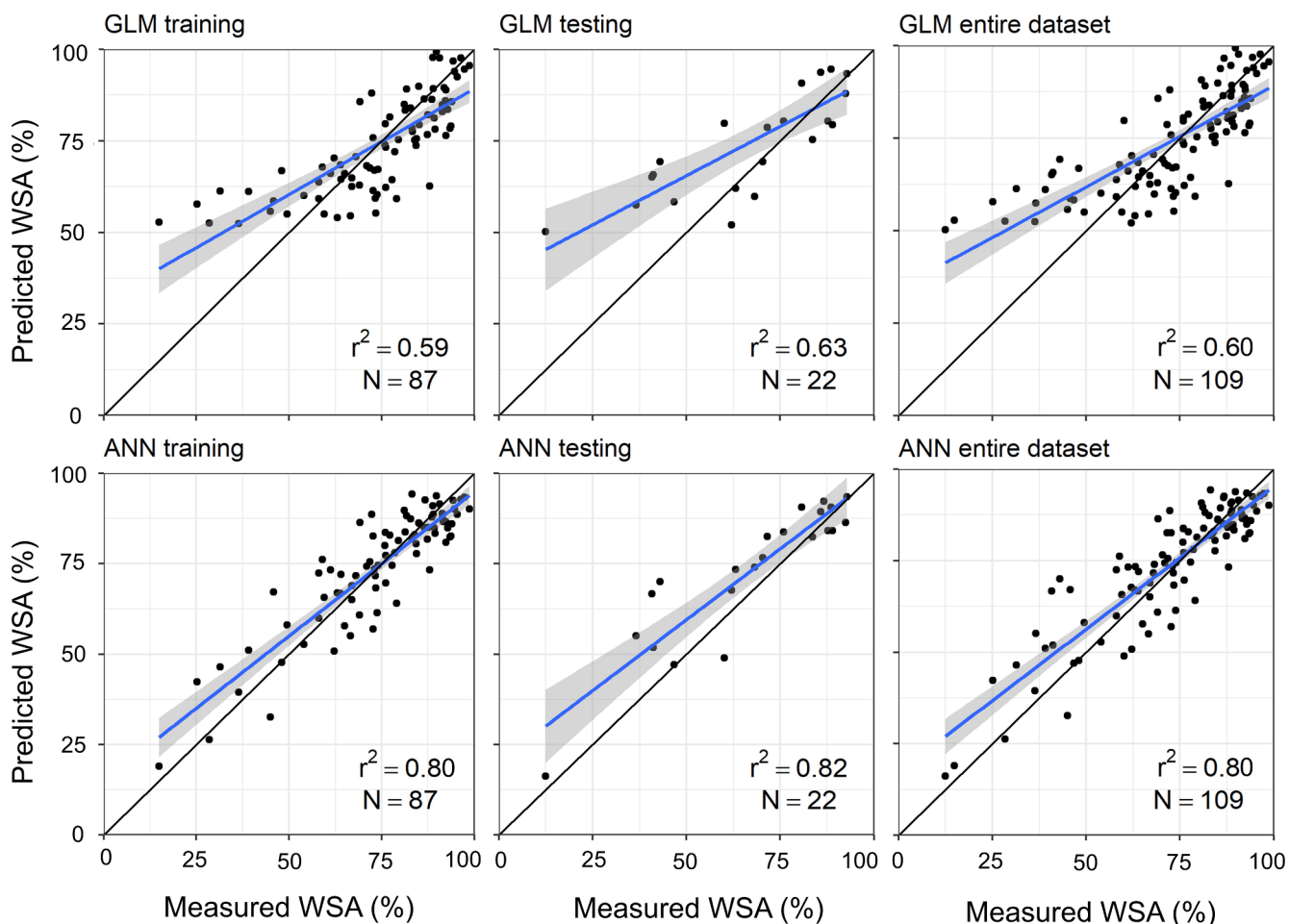


Fig. 6. Comparison between measured and predicted WSA values when using GLM and ANN models for training (80%), testing (20%), and entire dataset.

Table 3

Statistical summary of measured water-stable aggregates (WSA, %) used in cross-validation and testing.

	Mean	Standard deviation	Minimum	Maximum
Training (n = 87)	74.9	19.2	14.9	98.7
Testing (n = 22)	67.3	22.0	12.5	92.8

Declaration of Competing Interest

The authors declared that there is no conflict of interest.

Acknowledgments

This research was supported by funding from the National Commission for Scientific and Technological Research, Grant CONICYT/FONDECYT/Regular 1161045. The authors thank Dr. Paulina Ramírez for assistance with this research.

References

- Abiven, S., Menasseri, S., Angers, D.A., Leterme, P., 2008. A model to predict soil aggregate stability dynamics following organic residue incorporation under field conditions. *Soil Sci. Soc. Am. J.* 72, 119–125.
- Amézketa, E., 1999. Soil aggregate stability: a review. *J. Sustain. Agric.* 14, 83–151.
- Almajmaie, A., Hardie, M., Acuna, T., Birch, C., 2017. Evaluation of methods for determining soil aggregate stability. *Soil Tillage Res.* 167, 39–45.
- An, S.S., Mentler, A., Mayer, H., Blum, W.E., 2010. Soil aggregation, aggregate stability, organic carbon and nitrogen in different soil aggregate fractions under forest and shrub vegetation on the Loess Plateau, China. *Catena* 81, 226–233.
- Angers, D.A., Recous, S., Aita, C., 1997. Fate of carbon and nitrogen in water-stable aggregates during decomposition of $^{13}\text{C}^{15}\text{N}$ -labelled wheat straw *in situ*. *Eur. J. Soil Sci.* 48, 295–300.
- Annabi, M., Raclot, D., Bahri, H., Bailly, J.S., Gomez, C., Le Bissonnais, Y., 2017. Spatial variability of soil aggregate stability at the scale of an agricultural region in Tunisia. *Catena* 153, 157–167.
- Bazzoffi, P., Mbagwu, J.S.C., Chukwu, W.I.E., 1995. Statistical models for predicting aggregate stability from intrinsic soil components. *Int. Agrophys.* 9, 1–9.
- Belaid, H., Habaieb, H., 2015. Soil aggregate stability in a Tunisian semi-arid environment with reference to fractal analysis. *J. Soil Sci. Environ. Manage.* 6 (2), 16–23.
- Besalatpour, A., Ayoubi, S., Hajabbasi, M., Mosaddeghi, M., Schulin, R., 2013. Estimating wet soil aggregate stability from easily available properties in a highly mountainous watershed. *Catena* 111, 72–79.
- Besalatpour, A., Hajabbasi, M.A., Ayoubi, S., Gharipour, A., Jazi, A.Y., 2012. Prediction of soil physical properties by optimized support vector machines. *Int. Agrophys.* 26, 109–115.
- Bonilla, C.A., Vidal, K.L., 2011. Rainfall erosivity in Central Chile. *J. Hydrol.* 410, 126–133.
- Bonilla, C.A., Johnson, O.I., 2012. Soil erodibility mapping and its correlation with soil properties in Central Chile. *Geoderma* 189–190, 116–123.
- Bonilla, C.A., Pastén, P.A., Pizarro, G.E., González, V.I., Carkovic, A.B., Céspedes, R.A., 2014. Forest fires and water erosion effects on soil organic matter in the Serrano River basin (Chilean Patagonia). In: Hartemink, A., McSweeney, K. (Eds.), *Soil Carbon*, 2014 ed. Springer, Dordrecht 340 p.
- Bronick, C.J., Lal, R., 2005. Soil structure and management: a review. *Geoderma* 124 (1), 3–22.
- Cantón, Y., Solé-Benet, A., Asensio, C., Chamizo, S., Puigdefábregas, J., 2009. Aggregate stability in range sandy loam soils relationships with runoff and erosion. *Catena* 77, 192–199.
- Cañasveras, J.C., Barron, V., Del Campillo, M.C., Torrent, J., Gomez, J.A., 2010. Estimation of aggregate stability indices in Mediterranean soils by diffuse reflectance spectroscopy. *Geoderma* 158, 78–84.
- Carkovic, A.B., Pastén, P.A., Bonilla, C.A., 2015. Sediment composition for the assessment of water erosion and nonpoint source pollution in natural and fire-affected landscapes. *Sci. Total Environ.* 512–513, 26–35.
- Casanova, M., Salazar, O., Seguel, O., Luzio, W., 2013. The Soils of Chile. Springer, Dordrecht, pp. 110.

- Chaplot, V., Cooper, M., 2015. Soil aggregate stability to predict organic carbon outputs from soils. *Geoderma* 243–244, 205–213.
- Chenu, C., Le Bissonnais, Y., Arrouays, D., 2000. Organic matter influence on clay wettability and soil aggregate stability. *Soil Sci. Soc. Am. J.* 64, 1479–1486.
- Contreras, C.P., Bonilla, C.A., 2018. A comprehensive evaluation of pedotransfer functions for predicting soil water content in environmental modeling and ecosystem management. *Sci. Total Environ.* 644, 1580–1590.
- Deng, H., Fannon, D., Eckelman, M.J., 2018. Predictive modeling for US commercial building energy use: a comparison of existing statistical and machine learning algorithms using CBECS microdata. *Energy Build.* 163, 34–43.
- Devireni Saygm, S., Cornelis, W.M., Erpul, G., Gabriels, D., 2012. Comparison of different aggregate stability approaches for loamy sand soils. *Appl. Soil Ecol.* 54, 1–6.
- Dimoziannis, D., 2012. Wet aggregate stability as affected by excess carbonate and other soil properties. *Land Degrad. Dev.* 23, 450–455.
- Duchicela, J., Sullivan, T., Bonatti, E., Bever, J., 2013. Soil aggregate stability increase is strongly related to fungal community succession along an abandoned agricultural field chronosequence in the Bolivian Altiplano. *J. Appl. Ecol.* 50, 1266–1273.
- Erktan, A., Legout, C., De Danieli, S., Daumerge, N., Céclillon, L., 2016. Comparison of infrared spectroscopy and laser granulometry as alternative methods to estimate soil aggregate stability in mediterranean badlands. *Geoderma* 271, 225–233.
- Forkuor, G., Houmkpatin, O.K.L., Welp, G., Thiel, M., 2017. High Resolution mapping of soil properties using remote sensing variables in South-Western Burkina Faso: a comparison of machine learning and multiple linear regression models. *PLoS ONE* 12 (1).
- Gee, G.W., Bauder, J.W., 1986. Particle-size analysis. In: Klute, A. (Ed.), *Methods of Soil Analysis, Part 1. Physical and Mineralogical Methods*. American Society of Agronomy – Soil Science Society of America, Madison, WI, USA, pp. 383–411.
- Gomez, C., Le Bissonnais, Y., Annabi, M., Bahri, H., Raclot, D., 2013. Laboratory Vis–NIR spectroscopy as an alternative method for estimating the soil aggregate stability indexes of Mediterranean soils. *Geoderma* 209–210, 86–97.
- González, V.I., Carkovic, A.B., Lobo, G.P., Flanagan, D.C., Bonilla, C.A., 2016. Spatial discretization of large watersheds and its influence on the estimation of hillslope sediment yield. *Hydrol. Process.* 30, 30–39.
- Guisan, A., Edwards, T.C., Hastie, T., 2002. Generalized linear and generalized additive models in studies of species distributions: setting the scene. *Ecol. Model.* 157, 89–100.
- Günther, F., Fritsch, S., 2010. Neuralnet: training of neural networks. *R Journal* 2 (1), 30–38.
- Haghverdi, H., Öztürk, H.S., Durner, W., 2018. Measurement and estimation of the soil water retention curve using the evaporation method and the pseudo continuous pedotransfer function. *J. Hydrol.* 563, 251–259.
- Heung, B., Ho, H.C., Zhang, J., Knudby, A., Bulmer, C.E., Schmidt, M.G., 2016. An overview and comparison of machine-learning techniques for classification purposes in digital soil mapping. *Geoderma* 265, 62–77.
- Idowu, O.J., 2003. Relationships between aggregate stability and selected soil properties in humid tropical environment. *Commun. Soil Sci. Plant Anal.* 34 (5–6), 695–708.
- Igwe, C.A., Zarei, M., Stahr, K., 2009. Colloidal stability in some tropical soils of southeastern Nigeria as affected by iron and aluminium oxides. *Catena* 77, 232–237.
- INE, 2007. VII Censo Nacional Agropecuario y Forestal. Instituto Nacional de Estadística, Santiago, Chile.
- Karami, A., Homaei, M., Afzalinia, S., Ruhipour, H., Basirat, S., 2012. Organic resource management: impacts on soil aggregate stability and other soil physico-chemical properties. *Agric. Ecosyst. Environ.* 148, 22–28.
- Kemper, W.D., Rosenau, R.C., 1986. Aggregate stability and size distribution. In: Klute, A. (Ed.), *Methods of Soil Analysis, Part 1. Physical and Mineralogical Methods*. American Society of Agronomy–Soil Science Society of America, Madison, WI, USA, pp. 425–442.
- Krishnan, N.M.A., Mangalathu, S., Smedskjaer, M.M., Tandia, A., Burton, H., Bauchy, M., 2018. Predicting the dissolution kinetics of silicate glasses using machine learning. *J. Non-Cryst. Solids* 487, 37–45.
- Kuhn, M., 2018. A short introduction to the caret package. <https://cran.r-project.org/web/packages/caret/caret.pdf> (last accessed: 1/18/2019).
- Lagos-Avid, M.P., Bonilla, C.A., 2017. Predicting the particle size distribution of eroded sediment using artificial neural networks. *Sci. Total Environ.* 581–582, 833–839.
- Le Bissonnais, Y., 1996. Aggregate stability and measurement of soil crustability and erodibility: I. Theory and methodology. *Eur. J. Soil Sci.* 47, 425–437.
- Li, M.F., Tang, X.P., Wu, W., Liu, H.B., 2013. General models for estimating daily global solar radiation for different solar radiation zones in mainland China. *Energy Convers. Manage.* 70, 139–148.
- Luzio, W., Casanova, M., Seguel, O., 2010. Soils of Chile. In: Luzio, W. (Ed.), University of Chile. Maval Press, Santiago.
- Mataix-Solera, J., Benito, E., Andreu, V., Cerdà, A., Llovet, J., Úbeda, X., Martí, C., Varela, E., Gimeno, E., Arcenegui, V., Rubio, J.L., Campo, J., García-Orenes, F., Badía, D., 2010. ¿Cómo estudiar la estabilidad de agregados en suelos afectados por incendios? Métodos e interpretación de resultados. In: Cerdà, A., Jordán, A. (Eds.), Actualización en métodos y técnicas para el estudio de suelos afectados por incendios forestales. Cátedra de Divulgació de la Ciència. Universitat de València. FUEGORED 2010, Valencia, Spain, pp. 109–144.
- Mataix-Solera, J., Cerdà, A., Arcenegui, V., Jordán, A., Zavala, L.M., 2011. Fire effects on soil aggregation: a review. *Earth Sci. Rev.* 109, 44–60.
- McCullagh, P., Nelder, J.A., 1989. *Generalized Linear Models*, 2nd ed. Chapman and Hall, London.
- Minasny, B., Hartemink, A.E., 2011. Predicting soil properties in the tropics. *Earth-Sci. Rev.* 106, 52–62.
- Mohammadi, J., Motaghian, M.H., 2011. Spatial prediction of soil aggregate stability and aggregate-associated organic carbon content at the catchment scale using geostatistical techniques. *Pedosphere* 21 (3), 389–399.
- Nelson, D.W., Sommers, L.E., 1996. Total carbon, organic carbon, and organic matter. In: Sparks, D.L., Page, A.L., Helmke, P.A., Loepert, R.H., Soltanpour, P.N., Tabatabai, M.A., Johnston, C.T., Sumner, M.E. (Eds.), *Methods of Soil Analysis, Part 3: Chemical Methods*. Soil Science Society of America Inc, American Society of Agronomy Inc, Madison, WI, pp. 961–1010.
- Nciizah, A.D., Wakindiki, I.I.C., 2015. Physical indicators of soil erosion, aggregate stability and erodibility. *Arch. Agron. Soil Sci.* 61 (6), 827–842.
- Olden, J.D., Jackson, D.A., 2002. Illuminating the “black box”: a randomization approach for understanding variable contributions in artificial neural networks. *Ecol. Model.* 154 (1–2), 135–150.
- Onweremadu, E.U., Onyia, V.N., Anikwe, M.A.N., 2007. Carbon and nitrogen distribution in water-stable aggregates under two tillage techniques in Fluvisols of Owerri area, southeastern Nigeria. *Soil Tillage Res.* 97, 195–206.
- Paul, B., Vanlaue, B., Ayuke, F., Gassner, A., Hoogmoed, M., Hurisso, T., Koala, S., Lele, D., Ndabamenye, T., Six, J., 2013. Medium-term impact of tillage and residue management on soil aggregate stability, soil carbon and crop productivity. *Agric. Ecosyst. Environ.* 164, 14–22.
- Pulido Moncada, M., Gábris, D., Cornelis, W., Lobo, D., 2013. Comparing aggregate stability tests for soil physical quality indicators. *Land Degrad. Dev.* 26, 843–852.
- R Core Team, 2018. *R: A Language and Environment for Statistical Computing*. R Foundation for Statistical Computing, Vienna, Austria. <http://www.R-project.org/>.
- Rahmati, O., Tahmasebipour, N., Haghizadeh, A., Pourghasemi, H.R., Feizizadeh, B., 2017. Evaluation of different machine learning models for predicting and mapping the susceptibility of gully erosion. *Geomorphology* 298, 118–137.
- Ramírez, P.B., Calderón, F.J., Fonte, S.J., Bonilla, C.A., 2019. Environmental controls and long-term changes on carbon stocks under agricultural lands. *Soil Tillage Res.* 186, 310–321.
- Regelink, I.C., Stoof, C.R., Rousseva, S., Weng, L., Lair, G.J., Kram, P., Nikolaidis, N.P., Kercheva, M., Banwart, S., Comans, R.N., 2015. Linkages between aggregate formation, porosity and soil chemical properties. *Geoderma* 247, 24–37.
- Schutter, M.E., Dick, R.P., 2002. Microbial community profiles and activities among aggregates of winter fallow and cover-cropped soil. *Soil Sci. Soc. Am. J.* 66, 142–153.
- Six, J., Bossuyt, H., De Gryze, S., Denef, K., 2004. A history of research on the link between (micro) aggregates, soil biota, and soil organic matter dynamics. *Soil Tillage Res.* 79, 7–31.
- Shahbaz, M., Kuzyakov, Y., Heitkamp, F., 2017. Decrease of soil organic matter stabilization with increasing inputs: mechanisms and controls. *Geoderma* 304, 76–82.
- Tamari, S., Wösten, J.H.M., Ruiz-Suárez, J.C., 1996. Testing an artificial neural network for predicting soil hydraulic conductivity. *Soil Sci. Soc. Am. J.* 60 (6), 1732–1741.
- Tavares Filho, J., Feltran, C.T.M., Oliveira, J.F., Almeida, E., Guimarães, M.F., 2012. Atributos do solo determinantes para a estimativa do índice de estabilidade de agregados. *Pesquisa Agropecuária Brasileira* 47 (3), 436–441.
- Tisdall, J.M., Oades, J.M., 1982. Organic matter and water-stable aggregates. *J. Soil Sci.* 33, 141–163.
- Uribe, J.M., Cabrera, R., de la Fuente, A., Panque, M., 2012. *Atlas Bioclimático de Chile*. Universidad de Chile, Santiago, Chile.
- Weng, L., Vega, F.A., Van Riemsdijk, W.H., 2011. Competitive and synergistic effects in pH dependent phosphate adsorption in soils: LCD modeling. *Environ. Sci. Technol.* 45 (19), 8420–8428.
- Wösten, J.H.M., Pachepsky, Y.A., Rawls, W.J., 2001. Pedotransfer functions: bridging the gap between available basic soil data and missing soil hydraulic characteristics. *J. Hydrol.* 251, 123–150.
- Wright, S.F., Upadhyaya, A., 1998. A survey of soils for aggregate stability and glomalin, a glycoprotein produced by hyphae of arbuscular mycorrhizal fungi. *Plant Soil* 198, 97–107.
- Wu, X., Wei, Y., Wang, J., Wang, D., She, L., Wang, J., Cai, C., 2017. Effects of soil physicochemical properties on aggregate stability along a weathering gradient. *Catena* 156, 205–215.
- Xiao, H., Liu, G., Liu, P.L., Zheng, F.L., Zhang, J.Q., Hu, F.N., 2017. Developing equations to explore relationships between aggregate stability and erodibility in Ultisols of subtropical China. *Catena* 157, 279–285.
- Xu, C., Xu, X., Liu, M., Yang, J., Zhang, Y., Li, Z., 2017. Developing pedotransfer functions to estimate the S-index for indicating soil quality. *Ecol. Ind.* 83, 338–345.